LETTER • OPEN ACCESS

Uncertainty in land carbon budget simulated by terrestrial biosphere models: the role of atmospheric forcing

To cite this article: Lucas Hardouin *et al* 2022 *Environ. Res. Lett.* **17** 094033

View the article online for updates and enhancements.

ENVIRONMENTAL RESEARCH
LETTERS

LETTER

Uncertainty in land carbon budget simulated by terrestrial biosphere models: the role of atmospheric forcing

Lucas Hardouin[1,2] , Christine Delire[1,*] , Bertrand Decharme[1] , David M Lawrence[3] , Julia E M S Nabel[4,5] , Victor Brovkin[5] , Nathan Collier[6], Rosie Fisher[7] , Forrest M Hoffman[6] , Charles D Koven[8] , Roland Séférian[1] and Tobias Stacke[5]

[1] CNRM, Météo-France, CNRS, Université de Toulouse, Toulouse, France
[2] LEFE, Université de Toulouse, CNRS, Toulouse, France
[3] National Center for Atmospheric Research, Boulder, CO, United States of America
[4] Max Planck Institute for Biogeochemistry, Jena, Germany
[5] Max Planck Institute for Meteorology, Hamburg, Germany
[6] Oak Ridge National Laboratory, Oak Ridge, TN, United States of America
[7] CICERO Center for International Climate Research, Oslo, Norway
[8] Climate and Ecosystem Sciences Division, Lawrence Berkeley National Lab, Berkeley, CA, United States of America
[*] Author to whom any correspondence should be addressed.

E-mail: christine.delire@meteo.fr

Abstract

Global estimates of the land carbon sink are often based on simulations by terrestrial biosphere models (TBMs). The use of a large number of models that differ in their underlying hypotheses, structure and parameters is one way to assess the uncertainty in the historical land carbon sink. Here we show that the atmospheric forcing datasets used to drive these TBMs represent a significant source of uncertainty that is currently not systematically accounted for in land carbon cycle evaluations. We present results from three TBMs each forced with three different historical atmospheric forcing reconstructions over the period 1850–2015. We perform an analysis of variance to quantify the relative uncertainty in carbon fluxes arising from the models themselves, atmospheric forcing, and model-forcing interactions. We find that atmospheric forcing in this set of simulations plays a dominant role on uncertainties in global gross primary productivity (GPP) (75% of variability) and autotrophic respiration (90%), and a significant but reduced role on net primary productivity and heterotrophic respiration (30%). Atmospheric forcing is the dominant driver (52%) of variability for the net ecosystem exchange flux, defined as the difference between GPP and respiration (both autotrophic and heterotrophic respiration). In contrast, for wildfire-driven carbon emissions model uncertainties dominate and, as a result, model uncertainties dominate for net ecosystem productivity. At regional scales, the contribution of atmospheric forcing to uncertainty shows a very heterogeneous pattern and is smaller on average than at the global scale. We find that this difference in the relative importance of forcing uncertainty between global and regional scales is related to large differences in regional model flux estimates, which partially offset each other when integrated globally, while the flux differences driven by forcing are mainly consistent across the world and therefore add up to a larger fractional contribution to global uncertainty.

1. Introduction

During the last decade, about 45% of anthropogenic carbon dioxide (CO_2) emissions remained and accumulated in the atmosphere. Model- and observation-based studies suggest that the remaining term was shared among ocean (24%) and land (32%) since 1960 (Friedlingstein *et al* 2021). Together, the

contribution of the ocean and terrestrial CO_2 uptake nearly halves the increase in atmospheric CO_2, damping the pace of climate change (Canadell *et al* 2021). These sinks significantly increased since the middle of the 20th century, mainly due to the acceleration of the increase in CO_2 concentrations, caused by fossil fuel emissions. However, carbon uptake processes depend strongly on climate variability, especially for the terrestrial biosphere (Le Quéré *et al* 2009, DeVries *et al* 2019). While the ocean sink grew from $1.1 \pm 0.4\,\mathrm{PgC \cdot yr^{-1}}$ in the 1960s to $2.8 \pm 0.4\,\mathrm{PgC \cdot yr^{-1}}$ in 2011–2020, with an inter-annual variability of a few tenths of $\mathrm{PgC \cdot yr^{-1}}$, the land sink rose from $1.2 \pm 0.5\,\mathrm{PgC \cdot yr^{-1}}$ to $3.1 \pm 0.6\,\mathrm{PgC \cdot yr^{-1}}$, but with inter-annual variations up to $2\,\mathrm{PgC \cdot yr^{-1}}$ (Friedlingstein *et al* 2021).

Accurate evaluations of anthropogenic emissions, atmospheric CO_2 levels and carbon cycle perturbation are necessary to monitor, understand and predict climate change. The Global Carbon Project (GCP) has published an annual report since 2013 (Le Quéré *et al* 2013, 2014, Friedlingstein *et al* 2020, 2021) that quantifies the magnitude and uncertainty of the five major components of the global carbon budget: fossil fuel emissions (E_{FOS}), emissions from land use change (E_{LUC}), the growth rate of atmospheric CO_2 (G_{ATM}), the ocean sink (S_{OCEAN}) and the land sink (S_{LAND}). In earlier analyses provided by the GCP, the terrestrial carbon cycle simulated by the terrestrial biosphere models (TBMs, called by the authors Land Biosphere Models or Dynamical Global Vegetation Models) was not considered reliable enough to be used in the report to estimate the land carbon sink (Le Quéré *et al* 2009, Schaefer *et al* 2012, Todd-Brown *et al* 2013). The land sink S_{LAND} was hence diagnosed indirectly as the residual of the other terms. However, the methodology was updated in the 2017 global carbon budget (Le Quéré *et al* 2017), partly due to improvements in carbon cycle representation (Collier *et al* 2018, Lawrence *et al* 2019, Arora *et al* 2020, Davies-Barnard *et al* 2020), but also because of evidence of underestimation and uncertainty in the ocean sink variability (Landschützer *et al* 2015, DeVries *et al* 2017). The global land sink is now estimated by the multi-model mean of the TBM simulations, with the budget imbalance term, B_{IM}, representing residual uncertainty and/or unexplained aspects of the actual global carbon cycle.

To account for model construction, structural, and parametric uncertainty, as many as 17 TBMs were used to estimate S_{LAND} by (Friedlingstein *et al* 2020). Simulations were run using a unified land use change data set (LUH2; Hurtt *et al* 2020), global atmospheric CO_2 trend, and atmospheric climate forcing (CRUJRA; Harris 2019). Use of a single forcing dataset for climatic forcing, however, means that any model spread due to climate forcing data uncertainty

is not represented by the GCP ensemble. Yet, several studies have identified historical climate forcing as a large source of uncertainty in terrestrial carbon cycle modelling (Hicke 2005, Jung *et al* 2007, Poulter *et al* 2011, Bonan *et al* 2019, Lawrence *et al* 2019). Hicke (2005), for example, highlights important biases in net primary productivity (NPP) estimation while using different radiation datasets, and (Poulter *et al* 2011) conclude that atmospheric forcing results in a large uncertainty compared to land-cover datasets for NPP, heterotrophic respiration (Rh) and net ecosystem exchange. More recently, as part of the assessment and benchmarking of the Community Land Model version 5 (CLM5) (Lawrence *et al* 2019), climate forcing uncertainty was compared to model structure uncertainty using two forcing data sets (Global Soil Wetness Project 3 and CRUNCEP) and three versions of CLM (CLM4, CLM4.5, and CLM5) that differ markedly in their carbon cycle representation (Bonan *et al* 2019). The authors concluded that climate forcing is a large source of uncertainty in the global carbon cycle, especially for GPP, NPP and Rh, and to a lesser extent for Net Biome Productivity. However, this study was performed with different versions of a single model, and only two estimates of atmospheric climate forcing. Arguably therefore, the importance of atmospheric forcing on carbon cycle estimation by TBMs remain insufficiently explored, especially in the context of recent model structural improvements in the 6th Coupled Model Intercomparison Project (CMIP6) generation of models.

In this study, we used the output from the TBMs of three Earth System Models (ESMs) participating in the CMIP6. We performed an analysis of variance similar to Hawkins and Sutton (2009), Lovenduski and Bonan (2017), Bonan *et al* (2019)in order to quantify the relative uncertainty from atmospheric forcing, models and forcing-model interactions in carbon flux estimates made by TBMs. We used a combination of three TBMs from ESM and three atmospheric forcing datasets in our analysis. We present results for the major terrestrial carbon cycle fluxes; gross primary productivity (GPP), autotrophic respiration (Ra) and heterotrophic respiration (Rh), at global and regional scales. We also investigate estimates of CO_2 emissions from natural fires (fFire) and highlight their role in the calculation of the land carbon sink, before focusing on sources of uncertainty in the global net ecosystem productivity (NEP = GPP−Ra−Rh−fFire).

2. Methods

2.1. CMIP6 models and atmospheric forcings
We used the results of three TBMs of CMIP6 ESMs described in table 1, from the Land Surface, Snow and Soil moisture Model Intercomparison

Table 1. Model description.

Terrestrial biosphere model	Community Land model CLM5 (Lawrence *et al* 2019)	ISBA-CTRIP (Decharme *et al* 2019, Delire *et al* 2020)	JSBACH3.2 (Reick *et al* 2021)
Parent climate model	Community Earth system model CESM2 (Danabasoglu *et al* 2020)	CNRM-ESM2-1 (Séférian *et al* 2019)	MPI-ESM1.2-LR (Mauritsen *et al* 2019)
Simulation resolution	0.9° latitude by 1.25° longitude	T127 (∼1.4°)	T63 (∼1.9°)
Fire	Process-based (Li *et al* 2012, Li and Lawrence 2017)	Simple, based on GlobFirm (Thonicke *et al* 2001)	Mechanistic, SPITFIRE (Lasslop *et al* 2014)
Natural vegetation dynamics	No	No	Yes (Reick *et al* 2013)
Nitrogen cycle	Revised (Fisher *et al* 2019)	No	New (Goll *et al* 2017)
Plant hydrodynamics	(Kennedy *et al* 2019)	No	No
Soil carbon decompostion	Yes	Yes	New (Goll *et al* 2015)
Soil hydrology	Multilayer	Multilayer	Multilayer (Hagemann and Stacke 2015)
Other	Numerous updates to hydrology, snow, gas exchange and crops	Similar	Similar

Table 2. Atmospheric forcing description.

Name	Global soil wetness project (GSWP3) version 1.09 (Kim 2017)	CRUJRA[a] (Harris 2019)	Princeton (Sheffield *et al* 2006) v2.2
Time resolution	3 hourly	6 hourly	3 hourly
Covered period	1901–2014	1901–2018	1901–2012
Reanalysis used	20th Century Reanalysis version 2 (Compo *et al* 2011)	Japanese Reanalysis (JRA) by the Japanese Meteorological Agency (JMA)[b]	National Centers for Environmental Prediction (NCEP) reanalysis
Corrected by air temperature	Climate Research Unit Timeseries (CRU TS) v3.21	CRU TS v4.03	CRU TS v3.2
Precipitation	Global Precipitation Climatology Center (GPCC) v7	CRU TS v4.03	CRU, Global Precipitation Climatology Project and TRMM Multi-satellite Precipitation Analysis
Radiation	Surface Radiation Budget (SRB) datasets (downwelling radiation fluxes)	CRU TS v4.03	SRB
Use	LS3MIP	GCP	Hydrology

[a] Erroneously named CRUNCEP in CMIP6 simulations.
[b] http://hydro.iis.u-tokyo.ac.jp/GSWP3/.

Project (LS3MIP, Van den Hurk *et al* 2016) of CMIP6. For the three models, land use transitions are forced by the Land Use Harmonization 2 (LUH2) time series (Hurtt *et al* 2020). Those three models have been selected because they are the only ones that report output from three different atmospheric forcings and also share data for emissions from fire, on the Earth System Grid Federation archive.

Three climate forcing datasets were used to force the TBMs, according to the LS3MIP protocol. Atmospheric forcing consists of hourly to 6 hourly data on precipitation, short and long wave solar radiation, near surface air temperature, specific humidity, and wind speed. The three forcings described in table 2 have a 0.5° × 0.5° spatial resolution.

For reference, results of analysis of this set of model simulations with the International Land Model Benchmarking (ILAMB, Collier *et al* 2018) package are provided here: www.ilamb.org/land-hist/. ILAMB produces systematic evaluation (plots, summary tables, scoring) of model output against observations for a range of metrics including bias, RMSE, pattern correlation, annual cycle phase, and variable-to-variable comparisons. The version of ILAMB presented here assesses 22 land carbon, water, and energy cycle variables model variables against more than 50 observational datasets.

2.2. Analysis of variance

To statistically disaggregate the impacts of climate forcing, model choice and their interactions on relevant output variables, we performed an ANOVA. We analysed nine terrestrial carbon cycle simulations—three TBMs forced by three forcings—for the time period 1960–2012, chosen to coincide with the beginning of atmospheric carbon dioxide measurements in the 1960s, and the end of the Princeton dataset. We quantify relative uncertainty into three sources: models, atmospheric forcing differences and model-forcing interactions which measure the fact that models behave differently to different forcing product. Details can be found in the supplementary material.

3. Results

3.1. Global scale

We first investigated and compared the forcing data in order to highlight the main differences and similarities. The three forcings mostly agree on near surface air temperature, but they present large differences in specific humidity, incoming shortwave and longwave radiation, and windspeed (figure 1). Princeton has much higher specific (and relative—not shown) humidity than CRUJRA or GSWP3 in most parts of the world, except in desert areas. Additionally, specific humidity is generally greater with GSWP3 than with CRUJRA in tropical regions. CRUJRA also has higher shortwave and lower longwave incoming radiation than GSWP3 and Princeton, both having almost identical values. The precipitation forcing differs also with higher values for GSWP3, especially within the Arctic circle related to snowfall uncertainties.

We performed the analysis of variance on the global estimates of GPP, Ra, Rh, GPP–Ra–Rh, fFire and NEP (figure 2). The results illustrate a dominant role of the atmospheric forcing variation on global GPP estimates (figure 2(a)), with large differences between the multi-model mean values according to the forcings (about 15 PgC·yr^{-1}), with GSWP3 resulting in lowest GPPs for all three models, Princeton the highest GPPs, and CRUJRA in between. The discrepancies between the models for a given forcing are smaller, especially for CRUJRA and Princeton. Global GPP estimates of the ISBA-CTRIP and CLM5 models are very similar when forced with the CRUJRA forcing, and slightly differ when forced with GSWP3 or Princeton. The global GPP estimates of JSBACH are the largest with all three forcings and the difference with the two other models is the biggest with the GSWP3 forcing. However, the three models obtain very similar results with the Princeton atmospheric forcing. This suggests a general sensitivity of the models to an atmospheric variable that is different between Princeton's and the two other forcings, such as specific humidity (figure 1). These nine simulation results indicate a strong sensitivity of modelled GPP to climate forcing.
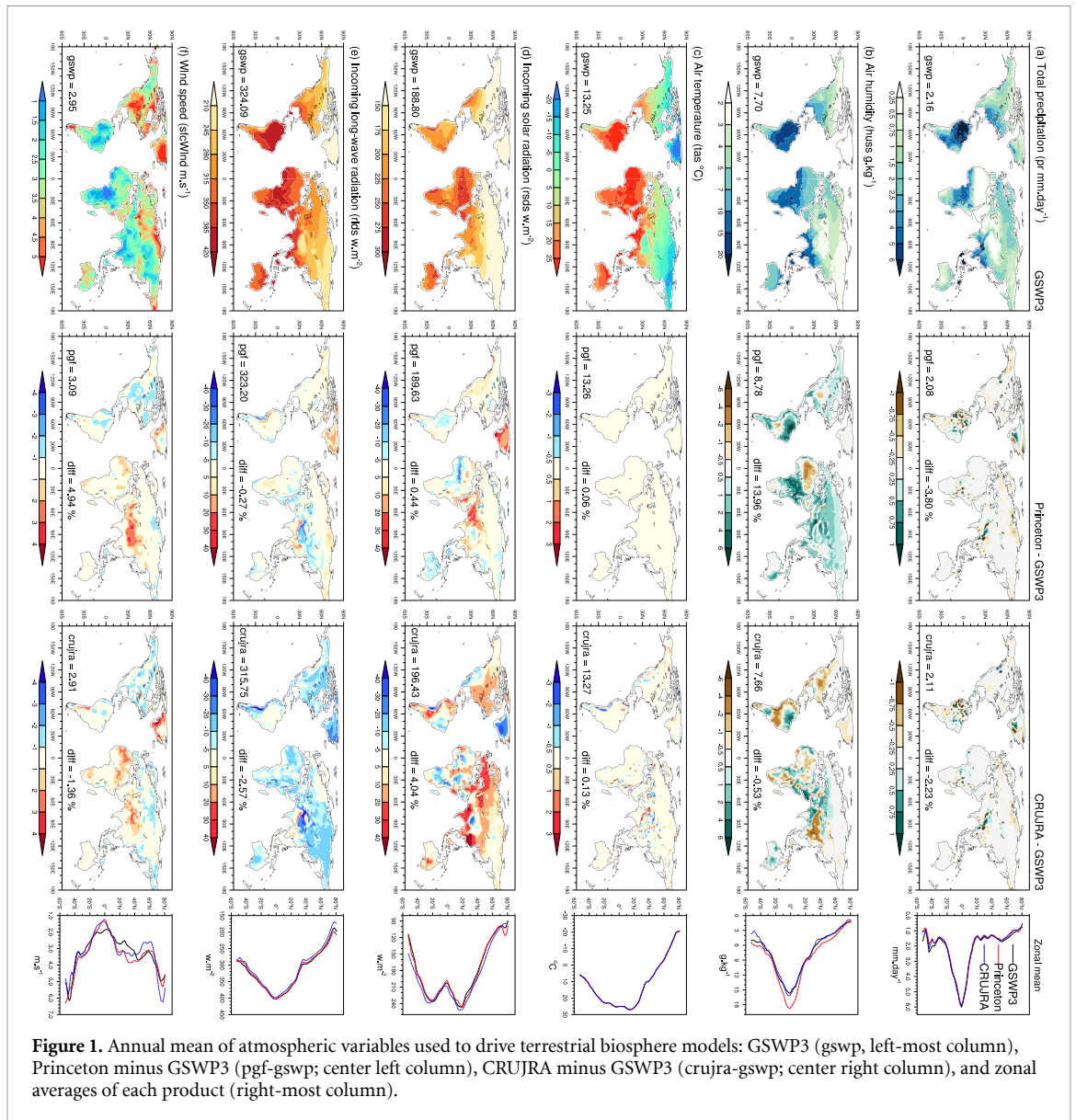
Figure 2(b) confirms the dominant role of atmospheric forcing on global GPP uncertainty. It accounts for ∼75% of the variability in the mean estimates, against ∼19% for models and ∼6% for interactions terms.

The dominance of atmospheric forcing contribution over the uncertainty is even more obvious for autotrophic respiration (figure 2(c)), again with similar model mean values for a given forcing but large differences between forcings with no overlap. According to our analysis of variance, ∼90% of the uncertainty can be assigned to forcings, ∼5% to models and ∼5% to the interactions terms (figure 2(d)). The Princeton forcing results in a slightly larger spread between the average autotrophic respiration than the other forcings.

Global NPP (GPP–Ra) behaves differently. Despite differences in multi-model mean values per atmospheric forcings (around 5 PgC·yr^{-1}) attesting to the role of forcing in uncertainty, we can see that JSBACH estimates are clearly higher than the two others (more than 10 PgC·yr^{-1}) in figure 2(e). This indicates greater model contribution to uncertainty, confirmed by figure 2(f) where models are the dominant source (∼63%) of uncertainty for NPP, but atmospheric forcing remains important with ∼30% of variability explained and ∼7% for model-forcing interactions. Contrary to ISBA-CTRIP and CLM5 that simulate the lowest NPP with GSWP3 and the highest with Princeton (like for GPP and Ra), JSBACH simulates a slightly smaller global NPP with the CRUJRA forcing. Global Rh presents similar results to global NPP (not shown), both for atmospheric contribution to uncertainty and for greater values obtained with GSWP3 than CRUJRA for JSBACH.
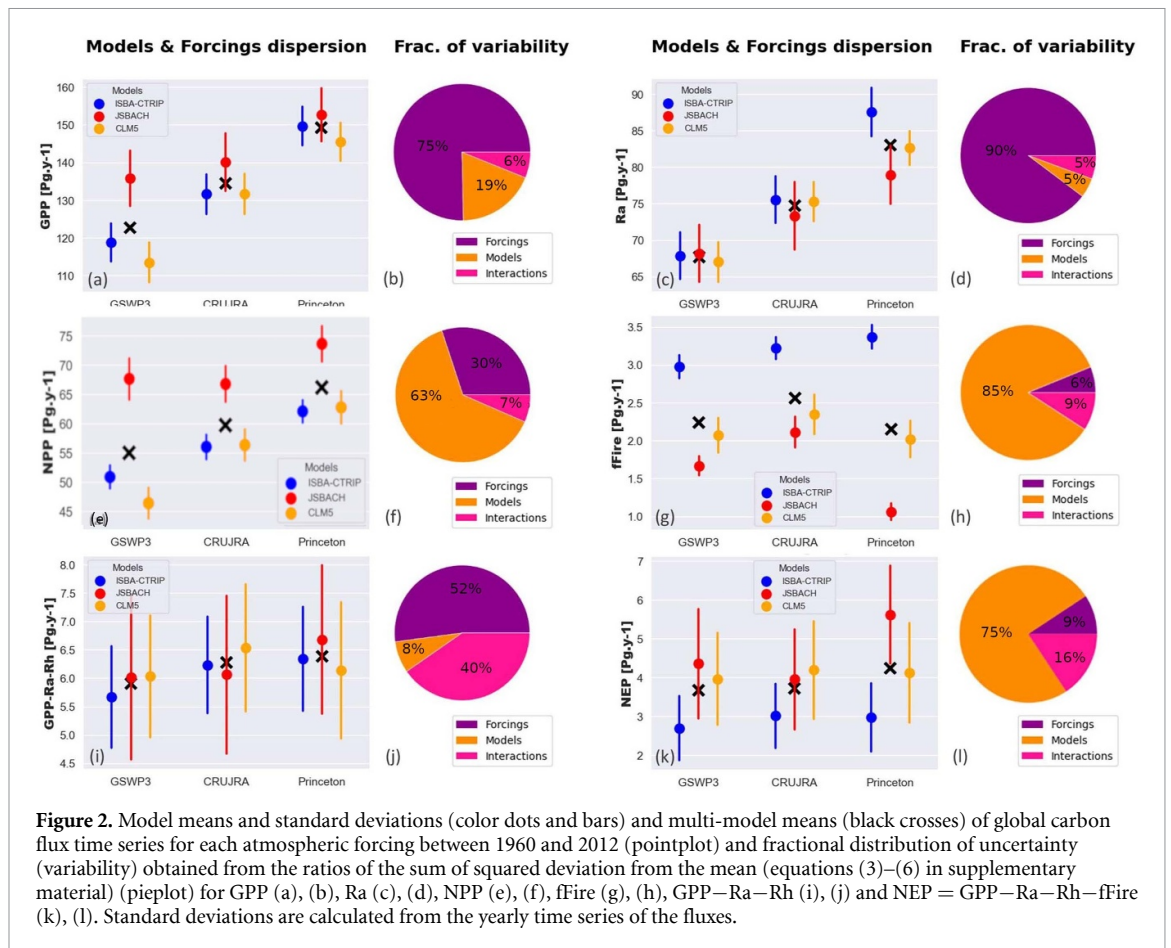
We show that atmospheric forcings have an important (NPP, Rh) and even dominant (GPP, Ra) role in uncertainty distribution for the major fluxes of global carbon cycle estimates. It seems that forcing contribution to uncertainty decreases when we consider net flux such as NPP and Rh rather than direct products of photosynthesis (GPP and Ra).

Wildfires are a small contribution to the global land carbon loss fluxes (∼2–3 PgC·yr^{-1}) (Van der Werf *et al* 2010), especially when compared to plant and soil respiration. Nonetheless, fire carbon losses correspond to approximately one-third of the GPP–Ra–Rh net flux. Moreover, this flux has particularly high seasonal and inter-annual variability, in response to both land cover change, as well as climatic events like drought. Despite its importance, anthropogenic biomass burning is not yet represented by all TBMs. Overall, high uncertainty remains in the carbon emissions associated with fire (figures 2(g) and (h)). ISBA-CTRIP tends to overestimate global

Figure 1. Annual mean of atmospheric variables used to drive terrestrial biosphere models: GSWP3 (gswp, left-most column), Princeton minus GSWP3 (pgf-gswp; center left column), CRUJRA minus GSWP3 (crujra-gswp; center right column), and zonal averages of each product (right-most column).

fire emissions compared to the global fire emission database (2.14 PgC·yr^{-1} for 1997–2015 van der Werf *et al*, 2017), while JSBACH is slightly lower (especially with Princeton). Part of these differences may be explained by the intermediate complexity fire module GlobFirm (Thonicke *et al* 2001) used in ISBA-CTRIP that is known to overestimate fire emissions (Li *et al* 2012). Figure 2(g) shows a large discrepancy between model values for a given forcing, particularly for the Princeton one, and figure 2(h) confirms a fractional contribution to uncertainty of ∼85% for the models, ∼6% for forcings and ∼9% for interactions. A closer look at fire results shows indeed interesting interactions between the forcings and fire modules that explain the bigger dispersion for Princeton. We saw that GPP and NPP (GPP–Ra) is enhanced with the Princeton forcing, most probably because of the high level of air humidity. For the GlobFirm module

implemented in ISBA-CTRIP, this leads simply to lower evapotranspiration rates, less moisture stress, higher productivity and litterfall (not shown) resulting in more biomass burned and greater associated carbon emissions. However, with the more mechanistic fire module of CLM5, the higher air humidity results directly in lower level of fuel flammability (see equation (8) Li *et al* 2012). In JSBACH, finally, the three applied forcings cause very different fire-vegetation feedbacks, such that the natural vegetation cover in the three simulations differs strongly, particularly in fire prone regions such as Africa and Asia (not shown). Such strong fire-vegetation feedbacks have already been observed for JSBACH in previous idealised model simulations (Lasslop *et al* 2016). Emissions from fire appear to be quite sensitive to atmospheric forcing when we compare individually the relative dispersion for each model,

Figure 2. Model means and standard deviations (color dots and bars) and multi-model means (black crosses) of global carbon flux time series for each atmospheric forcing between 1960 and 2012 (pointplot) and fractional distribution of uncertainty (variability) obtained from the ratios of the sum of squared deviation from the mean (equations (3)–(6) in supplementary material) (pieplot) for GPP (a), (b), Ra (c), (d), NPP (e), (f), fFire (g), (h), GPP−Ra−Rh (i), (j) and NEP = GPP−Ra−Rh−fFire (k), (l). Standard deviations are calculated from the yearly time series of the fluxes.

but this dependency is overshadowed in this analysis by the even larger uncertainty related to the model structure.

Here, we first present results for GPP–Ra–Rh estimates. This flux takes into account the most important and probably best represented processes of the terrestrial biosphere carbon sink, by excluding fire emissions. As expected, this net flux is smaller and has larger interannual variability (standard deviation) relative to the mean than the gross fluxes GPP, Ra and Rh. Figure 2(i) suggests a more important contribution to uncertainty by forcing than models: model mean values are close to each other for a given forcing and there is a small difference between forcings. The analysis of variance results shows effectively a dominant role of forcings (∼52%) over models (∼8%) but also a substantial contribution of the interaction terms (∼40%) (figure 2(j)). Indeed, the models do not show similar patterns with respect to the forcings. CLM5 results in greater values for CRUJRA (6.53 PgC·yr^{-1}) than Princeton (6.14 PgC·yr^{-1}), while ISBA-CTRIP simulates slightly bigger fluxes with Princeton (6.33 PgC·yr^{-1}) than with CRUJRA (6.23 PgC·yr^{-1}), as does JSBACH with a greater difference (6.06 for CRUJRA against 6.68 PgC·yr^{-1} with Princeton). In addition, we observe only slightly bigger results for CRUJRA than GSWP3 for JSBACH, consistent with

the results obtained from Rh and NPP, while the difference is more pronounced for ISBA-CTRIP and CLM5. This highlights differences in model sensitivity to atmospheric forcings, such as air humidity or downward radiation flux, for the land sink calculation.

Larger differences are obtained when we take into account fFire in the NEP calculation (figures 2(k) and (l)). There is only a small difference between the multi-model mean values per forcing, and a larger spread between the values of the different models, especially with the Princeton forcing (figure 2(k)). Moreover, global NEP is almost independent of the forcing with CLM5 and ISBA-CTRIP, which is not the case with JSBACH. The variance analysis results show that models contribute ∼75% to uncertainty, forcings account for ∼9% and interactions for ∼16%. This contrasts with the significant forcing contribution we obtained when not accounting for fFire, and indicates clearly a high model uncertainty related to fire emission.

To complete the global picture we analyze the contribution of atmospheric forcing to uncertainty in carbon stocks (figure 3). Atmospheric forcing plays a role in global carbon stock uncertainties but not a dominant one like for gross carbon fluxes. There are large differences in live (cVeg) and dead biomass (cLitter), and soil organic carbon content
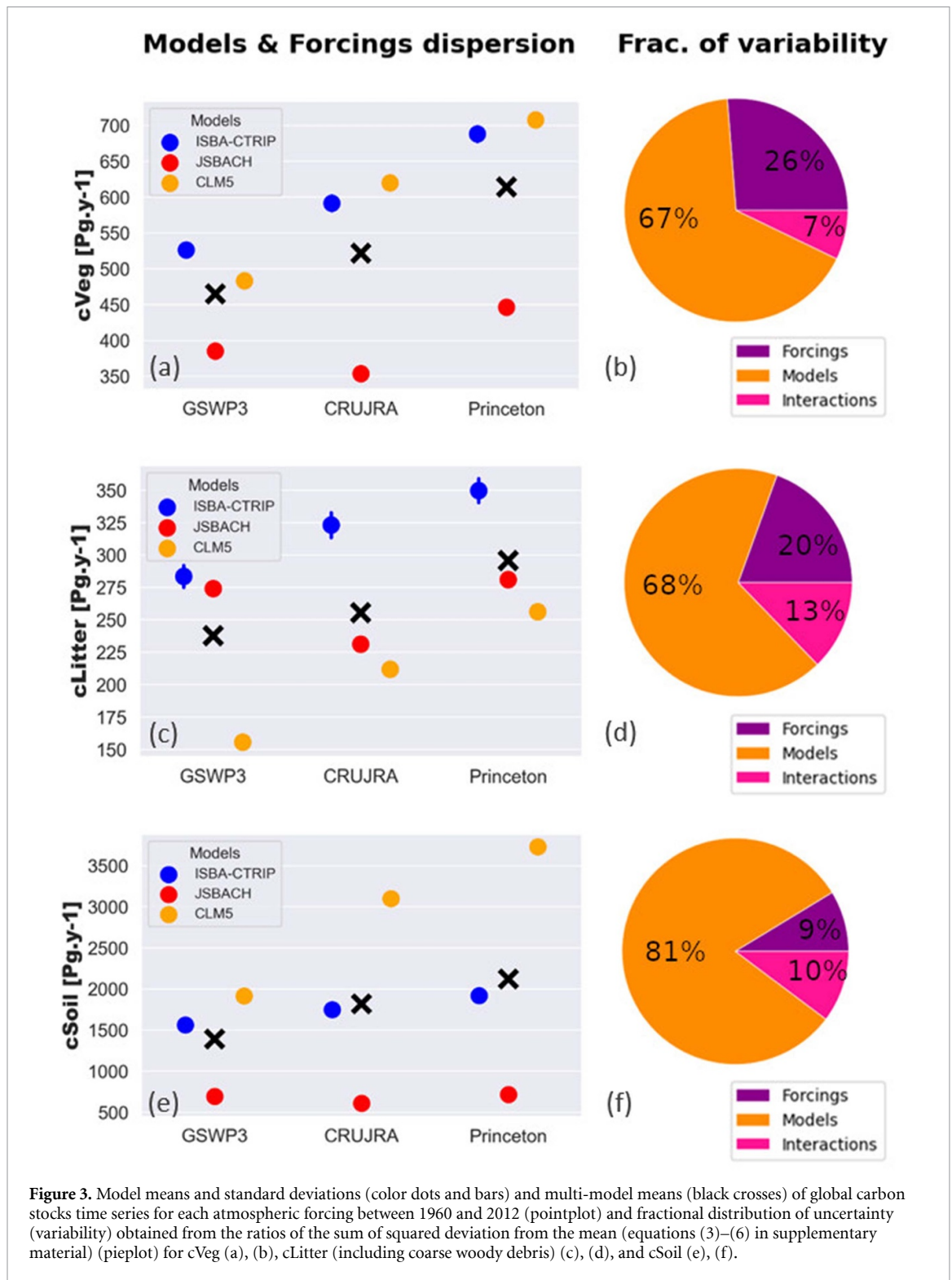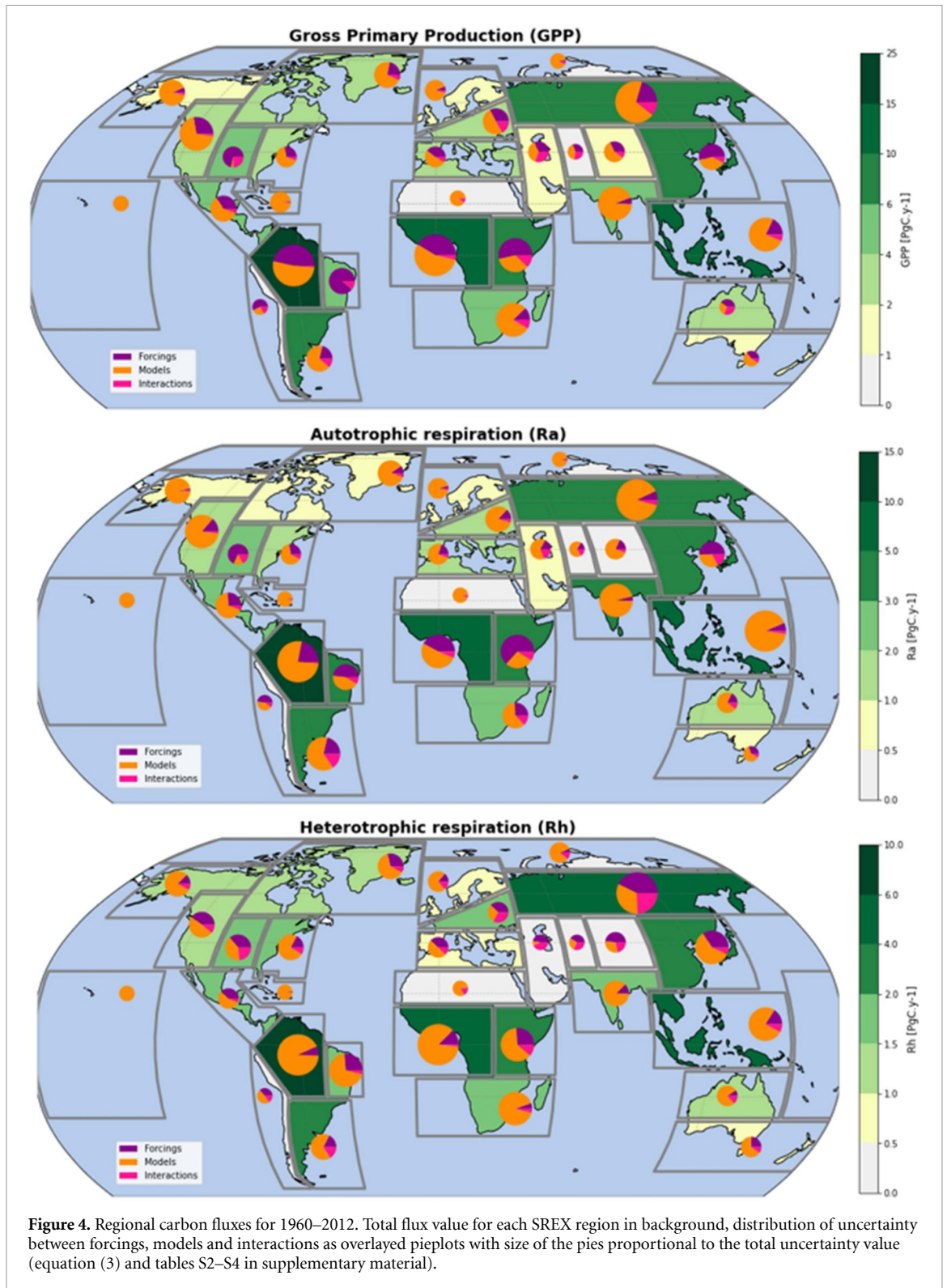
Figure 3. Model means and standard deviations (color dots and bars) and multi-model means (black crosses) of global carbon stocks time series for each atmospheric forcing between 1960 and 2012 (pointplot) and fractional distribution of uncertainty (variability) obtained from the ratios of the sum of squared deviation from the mean (equations (3)–(6) in supplementary material) (pieplot) for cVeg (a), (b), cLitter (including coarse woody debris) (c), (d), and cSoil (e), (f).

(cSoil) between multi-model means per forcing but the differences between models are even larger. The analysis of variance for cVeg shows that ∼26% of the uncertainty can be assigned to forcings, ∼67% to models and ∼7% to the interactions terms (figure 3(b)). For cLitter and cSoil, these numbers are respectively ∼20% and ∼9% for forcing, ∼68% and ∼81% for models and ∼13% and ∼10% for interactions (figures 3(d) and (f)). CLM5 and ISBA-CTRIP both simulate the smallest live and dead stocks with

GSWP3 while JSBACH simulates the smallest stocks with CRUJRA(figures 3(a), (c) and (e)). Princeton results in the largest stocks with every model. Live biomass from CLM5 and ISBA-CTRIP are fairly similar while JSBACH's is lower. The litter reservoir is the highest with ISBA-CTRIP and the lowest with CLM5 while the soil carbon is the largest with CLM5 especially for CRUJRA and Princeton. The higher soil carbon content with CLM5 can be explained by the vertically discretized soil carbon module with deeper

Figure 4. Regional carbon fluxes for 1960–2012. Total flux value for each SREX region in background, distribution of uncertainty between forcings, models and interactions as overlayed pieplots with size of the pies proportional to the total uncertainty value (equation (3) and tables S2–S4 in supplementary material).

soils (down to a maximum of 8.5 m). In the case of ISBA-CTRIP and JSBACH the soil carbon reservoir only represents the carbon in the first meter.

3.2. Regional scale

We performed the same analysis of variance on the 30 sub-continental regions defined in the Intergovernmental Panel on Climate Change (IPCC) Special Report on Managing the Risks of Extreme Events

and Disasters to Advance Climate Change Adaptation (SREX; IPCC SREX 2012). Figure 4 presents the results for GPP, Ra and Rh. The regions that present the largest uncertainty (largest pies) for GPP (figure 4(a) and supplementary tables S2–S4) are North Asia (NAS), the Amazon forest (AMZ), and to a lesser extent West Africa (WAF), South Asia (SAS), South East Asia (SEA), East Africa (EAF), South Africa (SAF), and West North America (WNA)

even if WNA contributes only 2–4 PgC·yr^{-1} to global GPP. Atmospheric forcing is a dominant source of uncertainty (more than half) in some regions that have fairly large contributions to the global total GPP flux, such as EAF and East Asia (EAS), but also in Central North America (CNA), West Coast South America (WSA), and North East Brazil (NEB). Atmospheric forcing is an important source of uncertainty (more than a third) in AMZ and WAF, tropical forest regions, which contribute greatly to global GPP. Generally, it seems that atmospheric forcings play an important role in tropical regions. Less important contribution in SAS and SEA could be explained by monsoon regimes that prevail on atmospheric forcing differences, but also by model resolution that could explain dominant model uncertainty in island regions (SEA but also Caribbean and Pacific Island Regions). Model-forcing interactions play a secondary but significant role in some regions such as NAS, WAF and South East South America (SSA) for the ones that contribute the most to global GPP.

Slightly different results can be observed for Ra (figure 4(b)). Atmospheric forcing contribution to uncertainty is lower in NAS and AMZ, as well as SEA and NEB. Generally, the forcing and interaction terms seem to play a less important role in Ra than in GPP regional estimates. For Rh (figure 4(c)), forcing contribution is even more reduced in tropical regions, where the fractional distribution never exceeds one-third. However, atmospheric forcing plays an important role in heterotrophic respiration uncertainty in the northern hemisphere's mid and high latitudes (about one-third). Interaction terms become also important in numerous mid and northern regions, particularly in NAS, CNA and Central Europe (CEU). An interpretation could be that models do not predict the same evolution for Rh in the areas where atmospheric variables are changing faster.

It is interesting to probe why atmospheric forcing accounts for more uncertainty at global than regional scale. We found that some differences between the forcings have the same impact on most of the world's area, while model differences induce strong regional uncertainty but not in the same manner everywhere. As an example, GPP estimates are slightly larger with Princeton than with CRUJRA or GSWP3 in all regions (see supplementary material figure S1), regardless of the model and add up to a large difference at global scale. This is consistent with the idea that the higher humidity in the Princeton dataset allows for higher photosynthetic rates for all models forced by it. Conversely, GPP estimates by ISBA-CTRIP and CLM5 appear to be similar at global scale, yet the regional analysis highlights strong opposition between tropical regions with higher GPP for ISBA-CTRIP compared to CLM5, and the northern hemisphere which has higher GPP in CLM5 compared to ISBA-CTRIP

(see supplementary material figure S2). This leads to a strong model contribution to uncertainty at regional scale, but those differences compensate each other globally.

4. Conclusion

The goal of this study was to evaluate the uncertainty related to the use of different global atmospheric forcing datasets in terrestrial carbon cycle modelling. We used nine CMIP6 simulations from three TBMs run with three different forcings to perform our analysis. First, we focused on global averages and found that atmospheric forcings are a dominant source of uncertainty compared to model choice for GPP and Ra, and contribute significantly to the overall uncertainty for Rh and NPP. The contribution of atmospheric forcing to the net fluxes uncertainty is reduced since positive effects of atmospheric forcings on photosynthesis are partially offset by enhancement in the respiration fluxes. We still found an important role of atmospheric forcing on GPP-Ra-Rh temporal mean estimates, but with important interaction terms that translate different model responses to climate variables. Important differences in fire modelling lead to a dominant role of models in NEP uncertainty, even on a global scale, despite a visible relationship and interactions between fire emission and climate forcings.

Secondly, we looked at the partitioning of uncertainty at the regional scale, with the purpose of identifying the regions where atmospheric forcings contribute the most to the variability of GPP, Ra and Rh. We showed that generally, the model structure is the dominant source of uncertainty regionally, in contrast to what we found globally. Atmospheric forcing contribution remains significant and even slightly dominant in some regions, notably in tropical forests for GPP and Ra and in mid and northern high latitudes for Rh, but regional discrepancies among the models are stronger. However, and in contrast with the forcings, it is not the same models that result in the biggest and lowest values everywhere. Those differences add up and offset each other, leading to closer results globally.

While the purpose of the study was to investigate the contribution of forcing uncertainty and to demonstrate the influence of choosing a specific forcing over another forcing, this experimental design, using three distinct sets of forcing data fields is not ideal for identifying the relative sensitivity to which drivers are most critical. While the large difference in humidity between Princeton and the other two datasets points to that field being particularly important in governing GPP and other fluxes, a more specific one-at-a-time propagation of the uncertainty in each field may allow for a more specific attribution of

uncertainty to meteorologic variables. Likewise, perturbations to the distributions while holding mean values constant may allow attribution of carbon cycle sensitivity to extremes. Nonetheless, these results point to a focus on constraining humidity values as key to reducing forcing uncertainty. To the extent that humidity is a key driver in GPP uncertainty, another question is whether this uncertainty is exacerbated in offline simulations such as used here, GCP, and elsewhere, because of the inability for surface moisture fluxes to attenuate humidity biases in the forcing fields due to the one-way coupling.

Additional work involving more TBMs and climate forcings should be done in order to better quantify the role of forcings in carbon cycle uncertainty, especially for the interactions between fire, land-cover dynamics and climate forcings. Even so, we conclude that atmospheric forcings are a key source of uncertainty in carbon cycle modelling at the global scale and are a significant source of uncertainty in some regions. Therefore, we suggest that where possible, it would be preferable for future MIPs and assessments (e.g. TRENDY, GCP, CMIP) to run simulations with several alternative climate forcing datasets, and to more specifically generate datasets to allow attribution of carbon cycle sensitivity both to uncertainty in meteorologic fields and to uncertainty in mean versus extreme values of meteorologic fields, when estimating the terrestrial carbon sink in order to correctly represent the uncertainty associated.

Data availability statement

The data that support the findings of this study are openly available at the following URL/DOI: https://esgf-node.llnl.gov/search/cmip6/.

Acknowledgments

ORCID iDs

Lucas Hardouin ● https://orcid.org/0000-0001-5226-0937
Christine Delire ● https://orcid.org/0000-0002-6114-3211
Bertrand Decharme ● https://orcid.org/0000-0002-8661-1464
David M Lawrence ● https://orcid.org/0000-0002-2968-3023
Julia E M S Nabel ● https://orcid.org/0000-0002-8122-5206
Victor Brovkin ● https://orcid.org/0000-0001-6420-3198
Rosie Fisher ● https://orcid.org/0000-0003-3260-9227
Forrest M Hoffman ● https://orcid.org/0000-0001-5802-4134
Charles D Koven ● https://orcid.org/0000-0002-3367-0065
Roland Séférian ● https://orcid.org/0000-0002-2571-2114
Tobias Stacke ● https://orcid.org/0000-0003-4637-5337

References

Arora V K *et al* 2020 Carbon–concentration and carbon–climate feedbacks in CMIP6 models and their comparison to CMIP5 models *Biogeosciences* **17** 4173–222

Bonan G B, Lombardozzi D L, Wieder W R, Oleson K W, Lawrence D M, Hoffman F M and Collier N 2019 Model structure and climate data uncertainty in historical simulations of the terrestrial carbon cycle (1850–2014) *Glob. Biogeochem. Cycles* **33** 1310–26

Canadell J *et al* 2021 Global carbon and other biogeochemical cycles and feedbacks *Climate Change 2021: The Physical Science Basis. Contribution of Working Group I to the Sixth Assessment Report of the Intergovernmental Panel on Climate Change* ed V Masson-Delmotte *et al* (Cambridge: Cambridge University Press)

Collier N, Hoffman F M, Lawrence D M, Keppel-Aleks G, Koven C D, Riley W J, Mu M and Randerson J T 2018 The international land model benchmarking (ILAMB) system: design, theory and implementation *J. Adv. Model. Earth Syst.* **10** 2731–54

Compo G P *et al* 2011 The twentieth century reanalysis project *Q. J. R. Meteorol. Soc.* **137** 1–28

Danabasoglu G *et al* 2020 The community earth system model version 2 (CESM2) *J. Adv. Model. Earth Syst.* **12** e2019MS001916

Davies-Barnard T *et al* 2020 Nitrogen cycling in CMIP6 land surface models: progress and limitations *Biogeosciences* **17** 5129–48

Decharme B *et al* 2019 Recent changes in the ISBA-CTRIP land surface system for use in the CNRM-CM6 climate model and in global off-line hydrological applications *J. Adv. Model. Earth Syst.* **11** 1207–52

Delire C *et al* 2020 The global land carbon cycle simulated with ISBA-CTRIP: improvements over the last decade *J. Adv. Model. Earth Syst.* **12** e2019MS001886

DeVries T *et al* 2019 Decadal trends in the ocean carbon sink *Proc. Natl Acad. Sci.* **116** 11646–51

DeVries T, Holzer M and Primeau F 2017 Recent increase in oceanic carbon uptake driven by weaker upper-ocean overturning *Nature* **542** 215–8

Fisher R A *et al* 2019 Parametric controls on vegetation responses to biogeochemical forcing in the CLM5 *J. Adv. Model. Earth Syst.* **11** 2879–95

Friedlingstein P *et al* 2020 Global carbon budget 2020 *Earth Syst. Sci. Data* **12** 3269–340

Friedlingstein P *et al* 2021 Global carbon budget 2021 *Earth Syst. Sci. Data* **14** 1–191

Goll D S, Brovkin V, Liski J, Raddatz T, Thum T and Todd-Brown K E 2015 Strong dependence of CO_2 emissions from anthropogenic land cover change on initial land cover and soil carbon parametrization *Glob. Biogeochem. Cycles* **29** 1511–23

Goll D S, Winkler A J, Raddatz T, Dong N, Prentice I C, Ciais P and Brovkin V 2017 Carbon–nitrogen interactions in idealized simulations with JSBACH (version 3.10) *Geosci. Model Dev.* **10** 2009–19

Hagemann S and Stacke T 2015 Impact of the soil hydrology scheme on simulated soil moisture memory *Clim. Dyn.* **44** 1731–50

Harris I 2019 CRU JRA v1. 1: a forcings dataset of gridded land surface blend of climatic research unit (CRU) and Japanese reanalysis (JRA) data, January 1901–December 2017 *University of East Anglia Climatic Research Unit, Centre for Environmental Data Analysis* (https://doi.org/10.5285/13f3635174794bb98cf8ac4b0ee8f4ed)

Hawkins E and Sutton R 2009 The potential to narrow uncertainty in regional climate predictions *Bull. Am. Meteorol. Soc.* **90** 1095–108

Hicke J A 2005 NCEP and GISS solar radiation data sets available for ecosystem modeling: description, differences and impacts on net primary production *Glob. Biogeochem. Cycles* **19** GB2006

Hurtt G C *et al* 2020 Harmonization of global land use change and management for the period 850–2100 (LUH2) for CMIP6 *Geosci. Model Dev.* **13** 5425–64

IPCC SREX 2012 *Managing the Risks of Extreme Events and Disasters to Advance Climate Change Adaptation. A Special Report of Working Groups I and II of the Intergovernmental Panel on Climate Change* ed C B Field *et al* (Cambridge: Cambridge University Press)

Jung M *et al* 2007 Uncertainties of modeling gross primary productivity over Europe: a systematic study on the effects of using different drivers and terrestrial biosphere models *Glob. Biogeochem. Cycles* **21** GB4021

Kennedy D, Swenson S, Oleson K W, Lawrence D M, Fisher R, Lola da Costa A C and Gentine P 2019 Implementing plant hydraulics in the community land model, version 5 *J. Adv. Model. Earth Syst.* **11** 485–513

Kim H 2017 Global soil wetness project phase 3 atmospheric boundary conditions (experiment 1) [data set] *Data Integration and Analysis System (DIAS)* (https://doi.org/10.20783/DIAS.50S)

Landschützer P *et al* 2015 The reinvigoration of the southern ocean carbon sink *Science* **349** 1221–4

Lasslop G, Brovkin V, Reick C H, Bathiany S and Kloster S 2016 Multiple stable states of tree cover in a global land surface model due to a fire-vegetation feedback *Geophys. Res. Lett.* **43** 6324–31

Lasslop G, Thonicke K and Kloster S 2014 Spitfire within the MPI earth system model: model development and evaluation *J. Adv. Model. Earth Syst.* **6** 740–55

Lawrence D M *et al* 2019 The community land model version 5: description of new features, benchmarking and impact of forcing uncertainty *J. Adv. Model. Earth Syst.* **11** 4245–87

Le Quéré C *et al* 2009 Trends in the sources and sinks of carbon dioxide *Nat. Geosci.* **2** 831–6

Le Quéré C *et al* 2013 The global carbon budget 1959–2011 *Earth Syst. Sci. Data* **5** 165–85

Le Quéré C *et al* 2014 Global carbon budget 2013 *Earth Syst. Sci. Data* **6** 235–63

Le Quéré C *et al* 2017 Global carbon budget 2017 *Earth Syst. Sci. Data* **10** 1–79

Li F and Lawrence D M 2017 Role of fire in the global land water budget during the twentieth century due to changing ecosystems *J. Clim.* **30** 1893–908

Li F, Zeng X and Levis S 2012 A process-based fire parameterization of intermediate complexity in a dynamic global vegetation model *Biogeosciences* **9** 2761–80

Lovenduski N S and Bonan G B 2017 Reducing uncertainty in projections of terrestrial carbon uptake *Environ. Res. Lett.* **12** 044020

Mauritsen T *et al* 2019 Developments in the MPI-M earth system model version 1.2 (MPI-ESM1. 2) and its response to increasing CO_2 *J. Adv. Model. Earth Syst.* **11** 998–1038

Poulter B, Frank D, Hodson E and Zimmermann N 2011 Impacts of land cover and climate data selection on understanding terrestrial carbon dynamics and the CO_2 airborne fraction *Biogeosciences* **8** 2027–36

Reick C H, Gayler V, Goll D, Hagemann S, Heidkamp M, Nabel J E M S *et al* 2021 *JSBACH 3 - The land component of the MPI Earth System Model: documentation of version 3.2* Hamburg: MPI für Meteorologie (https://doi.org/10.17617/2.3279802)

Reick C H, Raddatz T, Brovkin V and Gayler V 2013 Representation of natural and anthropogenic land cover change in MPI-ESM *J. Adv. Model. Earth Syst.* **5** 459–82

Schaefer K *et al* 2012 A model-data comparison of gross primary productivity: results from the north american carbon program site synthesis *J. Geophys. Res.: Biogeosci.* **117** G03010

Séférian R *et al* 2019 Evaluation of CNRM earth system model, CNRM-ESM2-1: role of earth system processes in present-day and future climate *J. Adv. Model. Earth Syst.* **11** 4182–227

Sheffield J, Goteti G and Wood E F 2006 Development of a 50-year high-resolution global dataset of meteorological forcings for land surface modeling *J. Clim.* **19** 3088–111

Thonicke K, Venevsky S, Sitch S and Cramer W 2001 The role of fire disturbance for global vegetation dynamics: coupling fire into a dynamic global vegetation model *Glob. Ecol. Biogeogr.* **10** 661–77

Todd-Brown K, Randerson J, Post W, Hoffman F, Tarnocai C, Schuur E and Allison S 2013 Causes of variation in soil carbon simulations from CMIP5 earth system models and comparison with observations *Biogeosciences* **10** 1717–36

Van den Hurk B *et al* 2016 LS3MIP (v1. 0) contribution to CMIP6: the land surface, snow and soil moisture model intercomparison project–aims, setup and expected outcome *Geosci. Model Dev.* **9** 2809–32

Van der Werf G R *et al* 2010 Global fire emissions and the contribution of deforestation, savanna, forest, agricultural and peat fires (1997–2009) *Atmos. Chem. Phys.* **10** 11707–35